Biophysical *Journal*
Article

Biophysical Society

The susceptibility of disulfide bonds to modification in keratin fibers undergoing tensile stress

Duane P. Harland,[1,*] Crisan Popescu,[2,3] Marina Richena,[1] Santanu Deb-Choudhury,[1] Claudia Wichlatz,[2] Erin Lee,[1] and Jeffrey E. Plowman[1]

[1]Smart Foods & Bioproducts, AgResearch, Ltd., Lincoln, New Zealand; [2]DWI, Aachen, Germany; and [3]Kao Germany GmbH, Darmstadt, Germany

ABSTRACT Cysteine residues perform a dual role in mammalian hairs. The majority help stabilize the overall assembly of keratins and their associated proteins, but a proportion of inter-molecular disulfide bonds are assumed to be associated with hair mechanical flexibility. Hair cortical microstructure is hierarchical, with a complex macro-molecular organization resulting in arrays of intermediate filaments at a scale of micrometres. Intermolecular disulfide bonds occur within filaments and between them and the surrounding matrix. Wool fibers provide a good model for studying various contributions of differently situated disulfide bonds to fiber mechanics. Within this context, it is not known if all intermolecular disulfide bonds contribute equally, and, if not, then do the disproportionally involved cysteine residues occur at common locations on proteins? In this study, fibers from Romney sheep were subjected to stretching or to their breaking point under wet or dry conditions to detect, through labeling, disulfide bonds that were broken more often than randomly. We found that some cysteines were labeled more often than randomly and that these vary with fiber water content (water disrupts protein-protein hydrogen bonds). Many of the identified cysteine residues were located close to the terminal ends of keratins (head or tail domains) and keratin-associated proteins. Some cysteines in the head and tail domains of type II keratin K85 were labeled in all experimental conditions. When inter-protein hydrogen bonds were disrupted under wet conditions, disulfide labeling occurred in the head domains of type II keratins, likely affecting keratin-keratin-associated protein interactions, and tail domains of the type I keratins, likely affecting keratin-keratin interactions. In contrast, in dry fibers (containing more protein-protein hydrogen bonding), disulfide labeling was also observed in the central domains of affected keratins. This central "rod" region is associated with keratin-keratin interactions between anti-parallel heterodimers in the tetramer of the intermediate filament.

SIGNIFICANCE The proteomic approach using alkylating labels and mass spectrometry allowed us to identify the location within protein chains (keratins and keratin-associated proteins) of disulfide bonds broken by tensile forces. Stretching the fibers when hydrogen bonds are disrupted affects interprotein interactions with the head domain of keratins with keratin-associated proteins and between the tail domains of keratins. Stretching the fibers when hydrogen bonds are unaffected affects interactions between heterodimers in the tetramers in the coiled domain.

INTRODUCTION

Keratin fibers, from hair and wool, are sophisticated multi-component and multi-scalar materials formed by a developmental process that includes biologically, chemically, and physically driven self-assembly processes (1,2). In addition to medical and subjective interest in human hair (3), there is the potential to biomimetically harness keratin material self-assembly processes to produce high-performing bio-based materials (e.g., plastic replacements) (4,5). A barrier to efforts in this context is the high level of internal molecular and structural complexity in hair which makes phenotypic expression, such as localized elastic properties, challenging to re-create during material development. Therefore, emerging approaches in reconstituted keratin (6) and other bio-based materials are increasingly turning to recreating mechanically functional aspects of native structure (7). Connecting macroscopic mechanical performance to its causation in molecular organization is termed mechanomics (8). Here, we report on mechanomic experiments investigating the location of mechanically relevant disulfide bonds across the microstructure of wool fibers (ovine hairs).

Submitted December 2, 2021, and accepted for publication April 25, 2022.

*Correspondence: duane.harland@agresearch.co.nz

Editor: Wendy J. Shaw.

https://doi.org/10.1016/j.bpj.2022.04.029

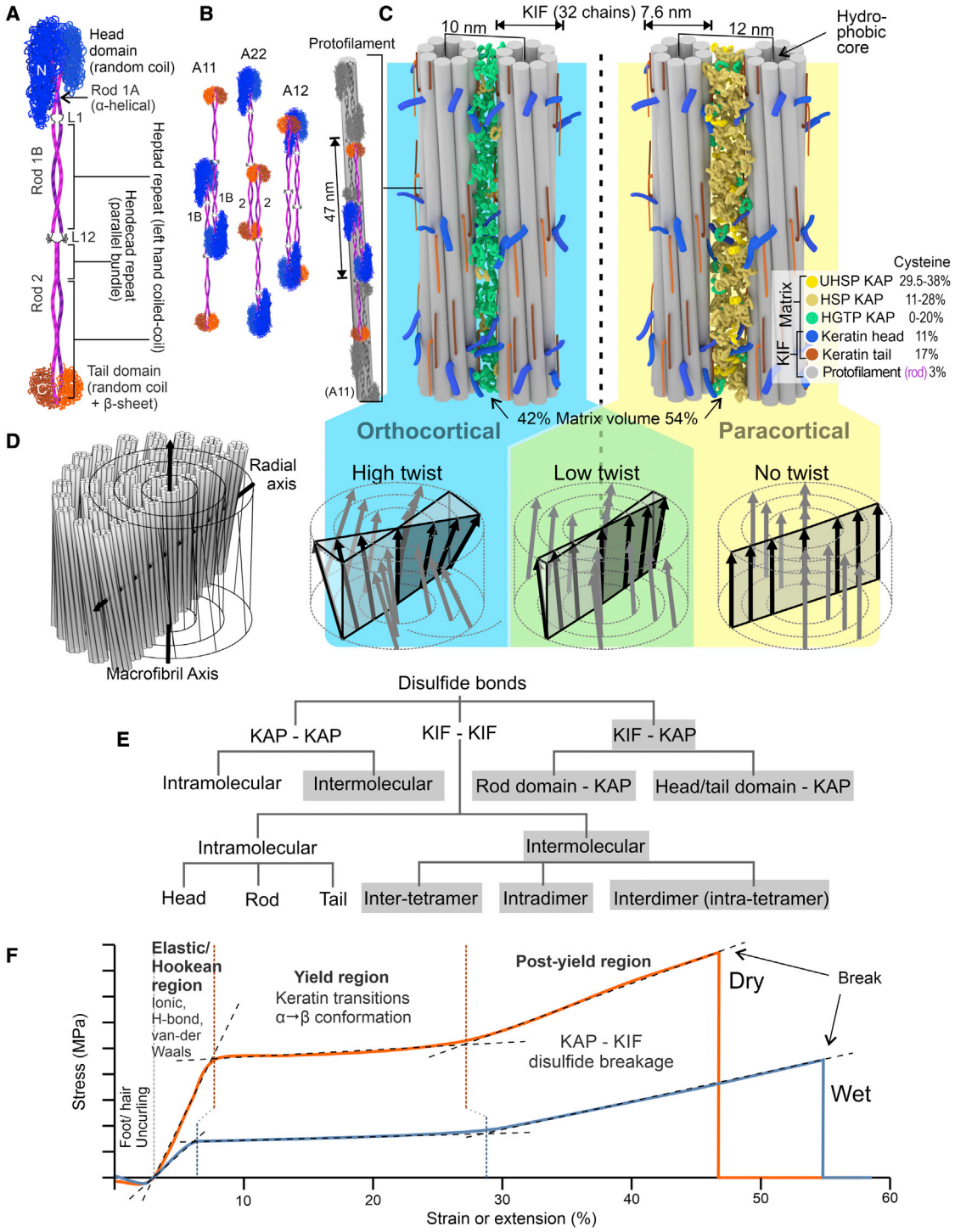

FIGURE 1 Protein structure and mechanical properties of hair cortex. (*A*) Trichokeratin type I, type II dimer. (*B*) Variants of dimer relationships in tetramers and one example of a protofilament from end-to-end tetramers, with A^{11} representing the interaction of rod 1 regions of the heterodimers, A^{22} the interaction of the rod 2 regions, and A^{12} the interaction between rods 1 and 2. (*C*) Intermediate filament arrangement, relationship with matrix, and differences between orthocortex and paracortex. (*D*) Example of double-twist macrofibril and variation in twist intensity across cortex. (*E*) Disulfide bonds between and within key fiber components with inter-structural disulfide bonds highlighted. (*F*) The tensile behavior of wet versus dry stretched fibers. KIF, keratin intermediate filament; L1 linker 1; N, amino-terminus; C, carboxy-terminus; L12, linker 1,2; HGTP, high glycine-tyrosine protein; HSP, high sulfur protein; UHSP, ultra-high sulfur protein; KAP, keratin-associated protein. To see this figure in color, go online.

Hairs develop within follicles via cellular-driven growth leading to programmed cell death that begins in a chemically reducing environment and progresses through a chemically oxidizing environment, ultimately culminating in hardening, cornification, and dehydration (9,10). Hair-shaft flexibility and its unique response to water are due to a chemical-bond network that stabilizes a multi-scalar organization of keratin and keratin-associated proteins (KAPs). Aside from the ionic and covalent bonds internal to proteins, hair or trichocyte keratins contain an unusually high level of disulfide bonds compared with epithelial keratins (11,12). In addition, the proximity of tightly packed protein chains within hair means that hydrogen bonds also play an important role in modulating mechanical performance (13–15).

During hair growth, the cortex (~90% of the volume of most fibers) undergoes an initial stage in which a progression of type I and II keratins are expressed (16,17) and form heterodimers (Fig. 1 *A*). The heterodimers associate into tetramers (Fig. 1 *B*), which then laterally associate into an eight-tetramer ring-like monomer (unit-length filament) and polymerize into keratin intermediate filaments (KIFs) such that the tetramers stack end to end to form protofilaments (Fig. 1 *B*) (18). Protofilaments form a ring surrounding a hydrophobic core, and it is thought that the cysteine-rich keratin head and tail domains (Fig. 1 *A*) largely decorate the outside of KIFs, protruding into the surrounding matrix, which is composed of keratin associate proteins (Fig. 1 *C*), and also project into the center of the protofilament to create a hydrophobic environment there (19). Composite bundles of KIFs and matrix, aligned with the fiber axis, are called macrofibrils (9). Macrofibrils are either crudely nematic (with no twist) or are double-twist structures (20) with inter-macrofibril variation in the intensity of the radial twist (Fig. 1 *D*) (21,22). All levels of structure are stabilized by disulfide bonds.

The matrix composition varies between macrofibril types. Orthocortical cell macrofibrils have KIFs that are more closely spaced (23), and the matrix is dominated by high glycine-tyrosine (HGT) KAPs, while KIFs in paracortical macrofibrils are more widely spaced and the matrix is dominated by high-sulfur (HS) and ultra-high-sulfur (UHS) KAPs (Fig. 1 *C*). The molecular and spatial organization of the matrix is poorly understood (24). During hair growth in the follicle, KIFs undergo an internal reorganization in an oxidizing environment, reducing the diameter from ~10 to ~7.5 nm. This transformation lines up cysteine residues to enable intra-KIF disulfide-bond formation (18), and, at about the same time, disulfide bonds between KIFs and KAPs and between KAPs and KAPs also form. The contribution of different classes of inter-protein connections within the disulfide-bond network within the KIF-matrix composite (Fig. 1 *E*) to the mechanical properties (e.g., tensile strength) of the hair shaft (Fig. 1 *F*) is the topic of this study.

Our hypothesis is that tensile-induced disulfide-bond breakage is not random and how easily a specific disulfide bond is broken by mechanical stress and how much that bond contributes to the overall fiber mechanics will depend on where it occurs within the keratin-KAP composite (Fig. 1 *E*). The null hypothesis is that all disulfide bonds contribute equally.

Hydrogen bonds between proteins are another factor affecting tensile behavior. They are more abundant than disulfide bonds in dry keratin fibers (one hydrogen bond and 1/9 disulfide bond per 122 molecular weight of keratin (14)), but the energy required to open a hydrogen bond (12–20 kJ/mol) is much lower than that for a disulfide bond (120–200 kJ/mol). The importance of hydrogen bonds in defining whole-hair-shaft tensile behavior is evident in the difference between the tensile behavior of wet compared with dry single hair fibers (Fig. 1 *F*). Water disrupts many of the protein-protein hydrogen bonds found in dry hair, and measurements of Young's modulus of longitudinally sectioned hair at various humidities using surface-probe nano-indentation has indicated that macrofibrils, and thus the KIF-KAP composite structure, is important in this context (15). Thus, water is a variable that affects how the proteins and bond network behave under mechanical stress.

Mechanical stresses that are harsh enough to break disulfide bonds may result in thiol-disulfide exchange with nearby cystines on stress release, but also cysteines can be lost to the bond network through oxidation events.

In this study, we used tensile stress and alkylating agents, which cap thiols resulting from broken disulfide

FIGURE 2 Plastic trays used to incubate wool fibers that had been mounted between plastic anchors in label and wash solution prior to stretching. The lower tray held the mounted hairs in an unstretched state, and the lid secured the anchors while allowing solutions access to the hairs.

bonds, to investigate the mechanical contribution of disulfide bonds in wet and dry contexts. This allowed us to examine differences in the mechanomics of hair supported by the disulfide-bond network alone and when additionally reinforced by the hydrogen-bond network.

MATERIALS AND METHODS

Sample origin and preparation

Wool fibers (mean diameter 33.0 μm ± 6.6 SD, measured by an optical fiber diameter analyzer [OFDA]) from a single Romney sheep were sourced from a farm in Barry's Bay, Canterbury, New Zealand. Staples of wool were de-tipped and scoured (washed) in 0.15% Teric GN9 in distilled water at 60°C and then 40°C, followed by washings in distilled water at 40°C and 60°C for 2 min in each condition (to simulate commercial scouring). The wool was the washed with dichloromethane, ethanol, and water to remove dirt and unbound lipids (25). Additional washes with dichloromethane were performed after air drying.

Fiber handling and tensile test conditions

The root-end 30 mm of 700 fibers were individually mounted between pairs of clip-together plastic tabs (Dia-Stron, Andover, UK) used to grip the fibers during stretching. All mounted fibers were placed in specially constructed plastic trays (Fig. 2) in which they could be immersed in solutions of the different alkylating agents and the wash solutions without individual handling of fibers.

Sets of 25 fibers were prepared, and each set was subjected to one of five experimental conditions: two wet conditions (conditions 1a and 1b), two dry conditions (conditions 2a and 2b), and a control that was not stretched but underwent all sample handling steps, as shown in Fig. 2. Conditions 1a, 1b, 2a, and 2b were repeated five times with separate sets of 25 fibers. The control was repeated seven times with separate sets of 25 fibers.

The four experimental conditions (Fig. 3) followed a similar sample-preparation protocol, with differences that facilitated variation in the water state of fibers (wet or dry) and two tensile conditions (stretched, held and relaxed, or stretched to break).

All samples were incubated in two alkylating agent labels at specific steps. Label A was 2 mM iodoacetamide (AppliChem GmbH, Darmstadt, Germany) in a 0.1 M sodium phosphate (Merck, Darmstadt, Germany) buffer and 1 mM EDTA (AppliChem GmbH, Darmstadt, Germany) made up in double-distilled

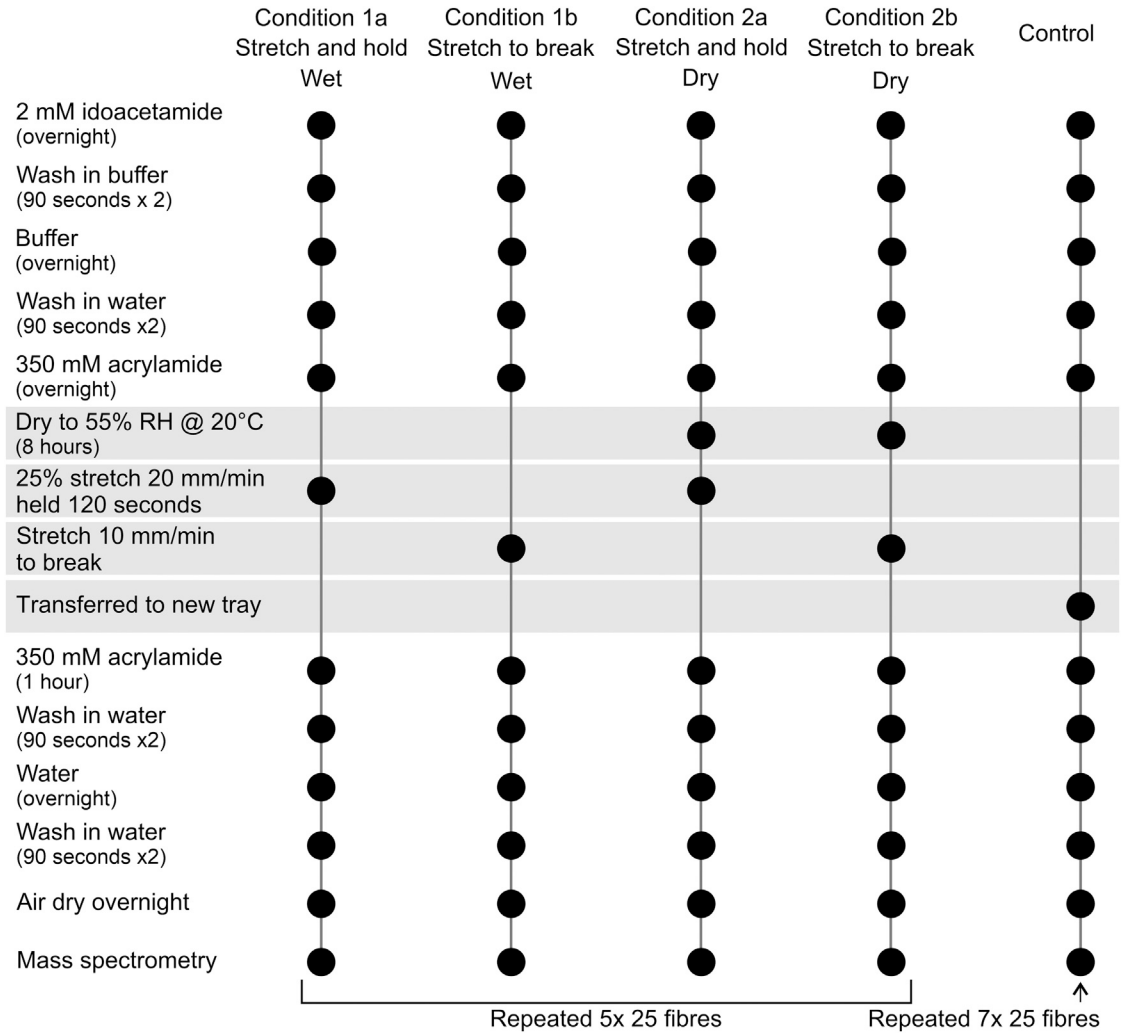

FIGURE 3 Summary of experimental sample protocol for all experimental conditions.

water to pH 7.4. Incubation in label A was carried out in the dark (closed laboratory cupboard). Label A's wash buffer was 1 mM EDTA in 0.1 M sodium phosphate buffer (pH 7.4). Label B was 350 mM acrylamide made up with double-distilled water, with a wash buffer that was double-distilled water. The process and timing for each label and wash is given in Fig. 2.

Tensile measurements were performed using a Dia-Stron Miniature Tensile Tester Model 675 (MTT675) with an attached Fiber Dimensional Analysis Unit Model 765 (FDAS765) (Dia-Stron). Depending on the condition, fibers were either stretched at 20 mm/min to 125% and then held for 120 s before being released or were stretched continuously at 10 mm/min until tensile failure. Samples subjected to wet testing were immersed in 350 mM acrylamide label upon loading into the sample carrousel. The carousel's plastic lid was secured to reduce contact between the label and the room atmosphere to minimize evaporation during the testing period.

Following tensile testing, all samples were transferred to a tray and immersed in fresh acrylamide label for 1 h before undergoing a washing process, before being left to air dry overnight. Dry fibers were individually removed from the tray, cut away from the plastic tabs, and accumulated into Eppendorf tubes for further processing by mass spectrometry.

Fiber digestion and mass spectrometry (MS) analysis

Accumulated fibers from each batch of 25 were digested with TPCK-trypsin at an enzyme:substrate ratio of 1:50 in 50 mM ammonium bicarbonate:AcN (9:1) for 18 h at 37°C. The resultant peptide digest was vortexed for 3 h in the presence of Empore disks, which had previously been prewetted with AcN, methanol, and water, following which the peptides were extracted with 75% AcN in 0.1% trifluoroacetic acid. The extracts were dried down on a Centrivap vacuum centrifugal concentrator (Labconco, Kansas City, MI, USA) and reconstituted in 0.1% trifluoroacetic acid.

MS using nanoflow-liquid chromatography and electrospray ionization was performed on a nanoAdvance UPLC coupled to an amaZon speed ETD mass spectrometer equipped with a CaptiveSpray source (Bruker Daltonik, Bremen, Germany). Sample aliquots (2 μL) were loaded onto a C18AQ nanotrap (Bruker)(2 cm × 75 μm, 3 μm particles, 200 Å pore size). The trap column was then switched in line with the analytical column (Bruker Magic C18AQ, 15 cm × 100 μm, 3 μm particles, 200 Å pore size). The column oven temperature was maintained at 50°C. A gradient from 0% to 40% B in 90 min at a flow rate of 800 nL/min was used for eluting the peptides. Solvent A was liquid chromatography-mass spectrometry (LCMS)-grade water with 0.1% formic acid and LCMS-grade 1% AcN; solvent B was 99% LCMS-grade AcN with 0.1% formic acid.

Automated information-dependent acquisition was performed using TrapControl (version 7.1, Build 83, Bruker, Billerica, MA, USA) software, with an MS survey scan over the range m/z 350–1200 followed by three MS/MS spectra from 50 to 3000 m/z acquired during each cycle of 30 ms duration.

Bioinformatics

Peak lists generated from each MS using nanoflow-liquid chromatography and electrospray ionization run were queried against *Ovis aries* in the NCBInr database (August 10, 2015) using the Mascot search engine (v2.4, Matrix Science, London, UK) maintained on an in-house server. The Mascot search parameters included semitrypsin as the proteolytic enzyme with two missed cleavages; error tolerance was set to 0.15 Da for MS and 0.3 Da for MS/MS. Variable modifications used were carbamidomethylation and propionamide. Search results were compiled and analyzed using ProteinScape 3.1.0 (Bruker) with the ProteinExtractor function. Acceptance thresholds for peptide and protein scores were set at 25 and 80, respectively. At least one peptide with a score indicating identity (as calculated by the search engine) was required for protein identification. Results assessed as being true matches were used for statistical analysis.

Statistical analysis

For each treatment condition, the two-sample Binomial exact test was used to compare whether the presence of individually labeled peptides occurred at a greater than random probability. This test was applied to each peptide that was not labeled in at least three of the seven unstretched (control) samples. Given the number of peptides and samples, three or greater occurrences was considered non-random at a confidence level of $p < 0.05$. This result was compared with the peptide's detection probability in five

TABLE 1 Peptides from which consistently labeled cysteines were detected in at least 3 out of 7 control samples (not stretched, 7 repeats)

Sequence	Protein ID	Position	Region
I^{116}LDELTLCK	K31	1B-70	
C^{42}GPCNSYVR	K31	T-42, T-45	tail domain
C^{42}GPCNSYVR	K31	T-42	tail domain
A^{7}VPAFSCVSACGPR	K81-like *Capra hircus*	H-13, H-17	head domain
A^{7}VPAFSCVSACGPR	K81-like *Capra hircus*	H-13	head domain
V^{475}GGSILGCK	K81-like *Capra hircus*	T-69	tail domain
T^{1}CGFSTVGSGFGSR	K83	H-2	head domain
C^{28}CITAAPYR	K83	H-28, H-29	head domain
C^{28}CITAAPYR	K83	H-28	head domain
D^{272}LNMDCIVAEIK	K83	2–4	coil 2
T^{16}FSSCSAVAPK	K85	H-20	head domain
S^{54}VSALGSCGPR	K85	H-61	head domain
D^{230}VDCAYLR	K85	1B-66	coil 1B
D^{284}LNMDCVVAEIK	K85	2–4	coil 2
G^{449}GVACGGLTYSSTAGR	K85	T-24	tail domain
Q^{162}CCESNLEPLFSGYIETLRR	K86	L1-5	linker 1
P^{119}TSCQPAPCR	KAP2.3 var2	22	
P^{119}TSCQPAPCR	KAP2.3 var2	27	
P^{119}TSCQPAPCR	KAP2.3 var2	22, 27	
L^{37}GCGYGCGYGYGSR	KAP6.1	39, 43	
L^{37}GCGYGCGYGYGSR	KAP6.1	43	
Y^{20}SGSSCGSSFPSNLVYR	KAP13.1	25	

treated samples against the detection probability of zero of the seven control samples. This resulted in peptides that were present in at least three treated samples being statistically significant ($p = 0.001$, 0.010, and 0.045 for peptides observed in five, four, and three treated samples, respectively).

RESULTS

Some cysteines were consistently labeled in the fibers in the control experiment (no stretching, repeated 7 times) (Tables 1 and S1), though not every cysteine in a multi-cysteine peptide was labeled, in contrast to the situation for the cysteines in the stretched samples (each condition repeated 5 times). A total of 84 unique sequences/peptides with labels (almost exclusively label A) were identified in all control and experimental samples. Only 43 sequences/peptides were not observed at all in any of 7 control samples, and this formed the basis for statistical comparisons. These peptides came from both keratins and KAPs. Of these peptides, 19 were found consistently in at least three of the five replicates compared with control samples, suggesting that there is a 95% probability that this was not by chance but due to one or more of the tensile treatments applied (Tables 2 and S1–S5).

TABLE 2 Peptides from the keratins and KAPs that contained consistently labeled cysteines and were detected in one or more of the 5 repeats of a treatment condition

	Significance/conditions							
	Wet		Dry (55% RH)					Fig. 8
Sequence	1a hold	1b break	2a hold	2b break	Protein ID	Position	Region	label
Consistently labeled cysteines irrespective of water and stretch conditions								
A^{489}SSFSCGSSR	5***	4**	5***	5***	K85	T-65	tail domain	A
C^{31}CISAAPYR	5***	5***	4**	3*	K85	H-31, H-32	head domain	A
Consistently labeled cysteines only when wet (hydrogen bonds disrupted) and both stretch conditions								
T^{12}GPATTICSSDKFCR	5***	4**	2	2	KAP3.2	19, 25	close to N-terminus	B
S^{98}SSCSSLSSGSR	4**	3*	2		KAP13.1 var1	102	in the middle (protein is 166 residues long)	B
G^{25}CGCGSFR	5***	3*	1		KAP19.5	26, 28	in the middle (protein is 72 residues long)	B
T^{380}ITPCISSPCAPAAPCTPCVPR	5***	5***	1	1	K31	T-22, T-27, T-33, T-36	close to C-terminus	B
S^{394}RFGPCNTSGC	5***	3*	2	1	K33b	T-37, T-42	C-terminal peptide	B
S^{53}VCGGFR	4**	3*	2	2	K83	H-55	head domain	B
V^{492}GGSILGCKK	5***	5***	2		K86-like	T-70	C-terminus but one, terminal cysteine	B
Consistently labeled cysteines when wet and stretched and held only								
L^{125}GYGICGFPVLSSGSGFCQPTFFASR	4**				KAP13.1 var1	130	close to the C-terminus (protein is 166 residues long)	C
T^{124}FRTSPCC	3*	2			KAP2.3 var3	130, 131	C-terminal peptide	C
T^{12}GPATTICSSDKF	3*		1		KAP3.2	19	close to N-terminus	C
Consistently labeled cysteines only in dry condition (reinforcing hydrogen bonds present) and both stretch conditions								
Y^{306}SCQLSQVQSLIVNVESQLAEIR			3*	3*	K31, K33b	2-90	coil 2B	D
Consistently labeled cysteines when dry and stretched and held only								
V^{179}ESLKEELICLK			3*	1	K31 var1, K33B	1B-87	coil 1B (seq. number for K31)	E
V^{179}ESLKEELLCLK			3*	1	K34	1B-87	coil 1B	E
Y^{306}SCQLNQVQSLISNVESQLAEIR			3*	2	K31, K33b	2-90	coil 2B	E
Consistently labeled cysteines only in stretch and hold condition but both wet and dry								
S^{121}ISTVCQPVGGVSTICQPTCGVSR	5***	2	3*		KAP11.1	126, 136, 140	close to the C-terminus (residue 158)	F
Consistently labeled cysteines only when fiber stretched to break and dry								
A^{214}DLEAQVESLKEELLCLK			1	3*	K35	1B-87	coil 1B	G
Consistently labeled cysteines in wet (both stretch conditions) and in dry stretched and held but not when dry stretched to break								
C^{395}GPCNTFVH	3*	3*	3*	2	K33a	T-33, T-36	tail domain	H

Statistical likelihood is marked as: *$p < 0.05$; **$p < 0.01$; ***$p < 0.001$.

Of the cysteines that were consistently labeled under all experimental conditions, three were from one type II keratin, K85, with two cysteines, H-31 and H-32, being in the head domain and the other, T-65, in the tail domain (Table 2 *A*, Fig. 4 *B*). These three disulfides were consistently labeled irrespective of the extra stabilizing influence of hydrogen bonds or whether the fiber was rapidly stretched to break or was given a longer but less severe stretch.

The effect of wet versus dry conditions

Conditions 1a and 1b were tested under wet conditions (stretch 25% and hold or break) and samples in conditions 2a and 2b were tested at 55% relative humidity (stretch or break). Disulfides that were consistently labeled in the wet state, when hydrogen bonds were disrupted, came from peptides found in both keratins and KAPs (Table 2 *B*; Fig. 5). What is notable about the keratin data is that all disulfides identified were from the head or tail domains. This included disulfides from the head domain of K83 (H-55) and the tail domains of K31 (T-22, T-27, T-33, and T-35), K33b (T-33 and T-36), and K86-like (T-70). In contrast, disulfides that were consistently labeled in the dry state when reinforcing hydrogen bonds were present were from the coil domains, specifically cysteines from Coil 1B in K31 var1 and K34 (1B-87), and coil 2B in K31 and K33b (2B-90) (Table 2 *D* and *E*; Fig. 6 *A–C*).

The effect of hold at 25% versus break

A number of cysteines were observed to be labeled when stretched to 25% but not when stretched to break. Among them were three cysteines in KAP11.1, where disulfide labeling occurred under both wet and dry conditions (Table 2 *F*; Fig. 6 *D*). In a further three KAPs, specifically KAP3.2, KAP2.3 var 3, and KAP13.1 var 1, cysteines were only labeled when stretched to 25% in the wet state (Table 2 *C*; Fig. 7). In contrast, stretching to 25% under dry conditions only labeled cysteines in the coil domains of keratins, specifically K31, K33b, and K34 (Table 2 *E*).

Other conditions

Two disulfide-linked cysteines in the tail domain of K33a were labeled in all conditions except when stretched to break under dry conditions (Table 2 *H*). One cysteine in coil 1B in K35 was only labeled when the fiber was stretched to break in the dry state (Table 2 *G*).

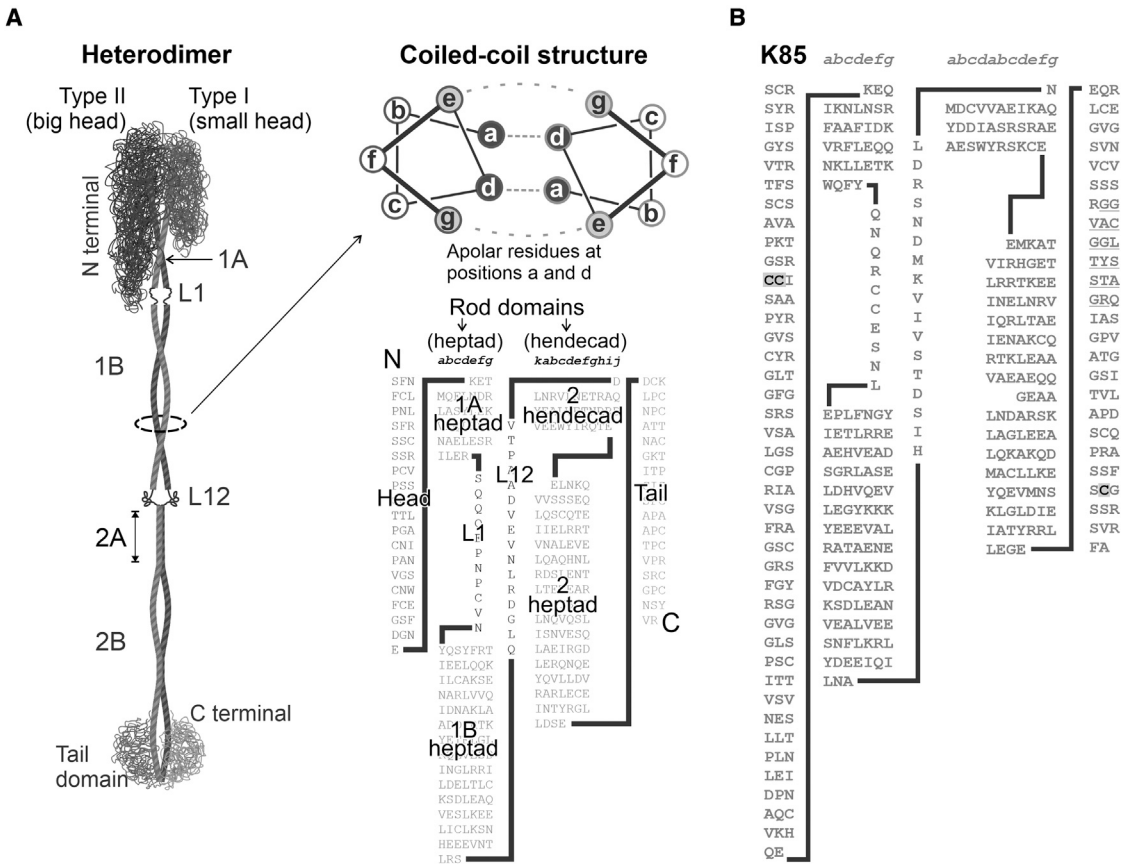

FIGURE 4 Trichokeratin intermediate filament heterodimers. (*A*) Key to relate sequence results to dimer structure. (*B*) K85 indicating consistently labeled disulfides highlighted and in bold.

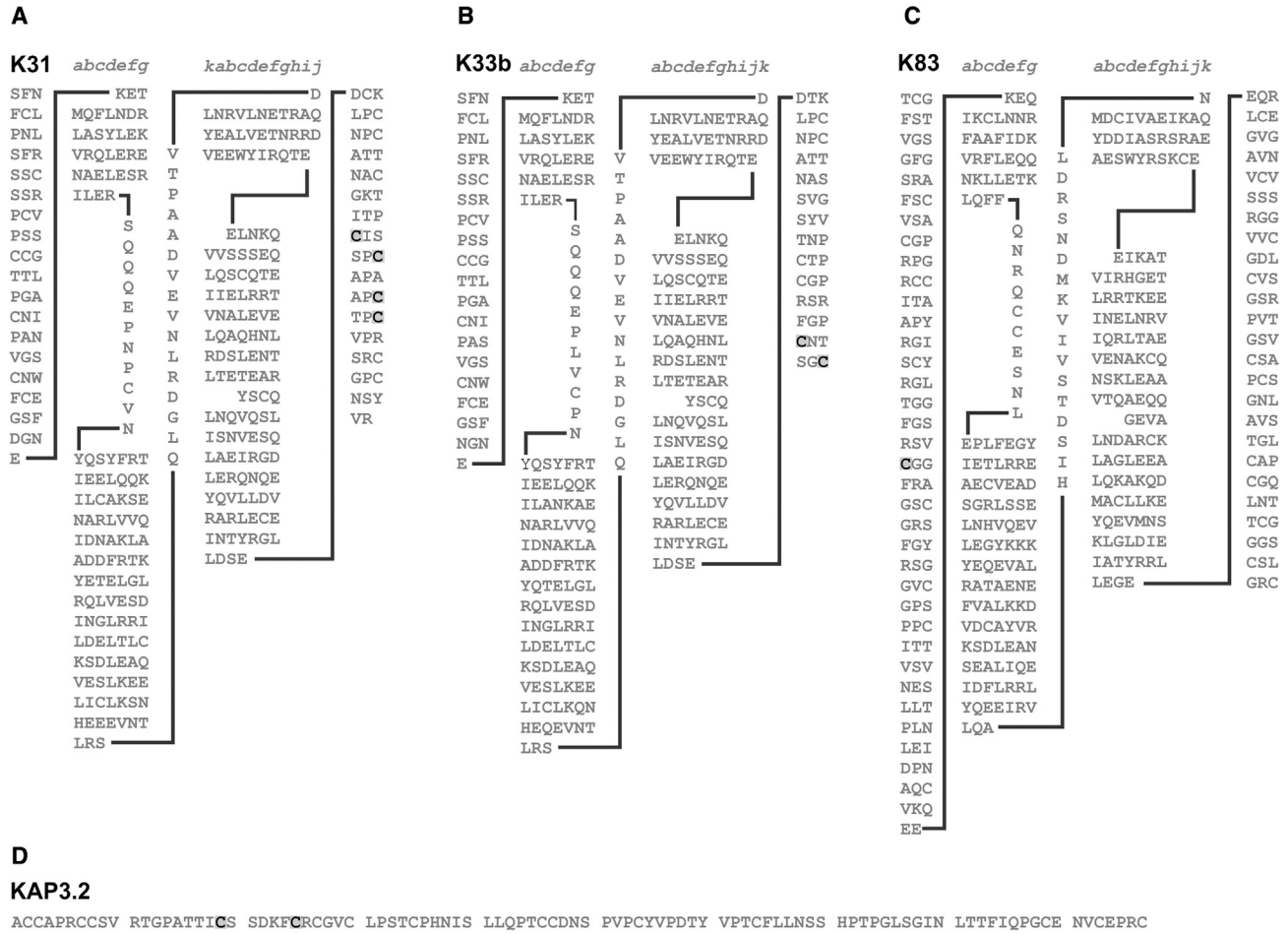

FIGURE 5 Some keratins and KAPs in which labeling occurred consistently in wet conditions only. (*A*) K31. (*B*) K33b. (*C*) K83. (*D*) KAP 3.2. Labeled cysteines are highlighted and in bold.

DISCUSSION

Disulfide labeling during tensile stress is not random

The key finding of this study is that disulfide labeling in wool fibers during the process of stretching or breaking the fiber is not random but disproportionately affects the cysteines at specific sites on keratins and KAPs (Fig. 8). Our method identifies this disproportionality against the background of random disulfide labeling that is also likely occurring within stressed fibers. Effectively, it identifies those cysteines that form weak points in the disulfide-bond network that are readily accessible to water. Conversely, labeling of the cysteines in the hydrophobic core of the 8 + 0 KIF is less likely to occur because of water-accessibility issues (19). Although the individual bonds themselves are no weaker at these points, the local molecular organization (intra- and inter-keratin/KAP quaternary structure) probably generates a disproportionate effect of strain at the molecular level at these points.

Non-random cysteine labeling was found in the control samples that had not undergone tensile stress. These may represent free thiols naturally present in the wool sample used or could be a result of single-fiber handling during experiments (handling steps occurred with controls, and only stretching was omitted). We consider that handling is the most likely explanation because in the control, only single labels were typically detected on peptides with multiple cysteines, and two previous studies using similar labeling chemistry but excluding most of the single-fiber handling steps (26,27) did not detect free thiols.

Keratin 85's head and tail domains contain key disulfides

The disulfides that showed consistent labeling under all stretching conditions were on K85 (Table 2 *A*; Fig. 4 *B*), which is found in both the cortex and cuticle, and is the first type II keratin to be expressed in the follicle (28). As these cysteines were found on either the head or tail domain, all would potentially be positioned to interact

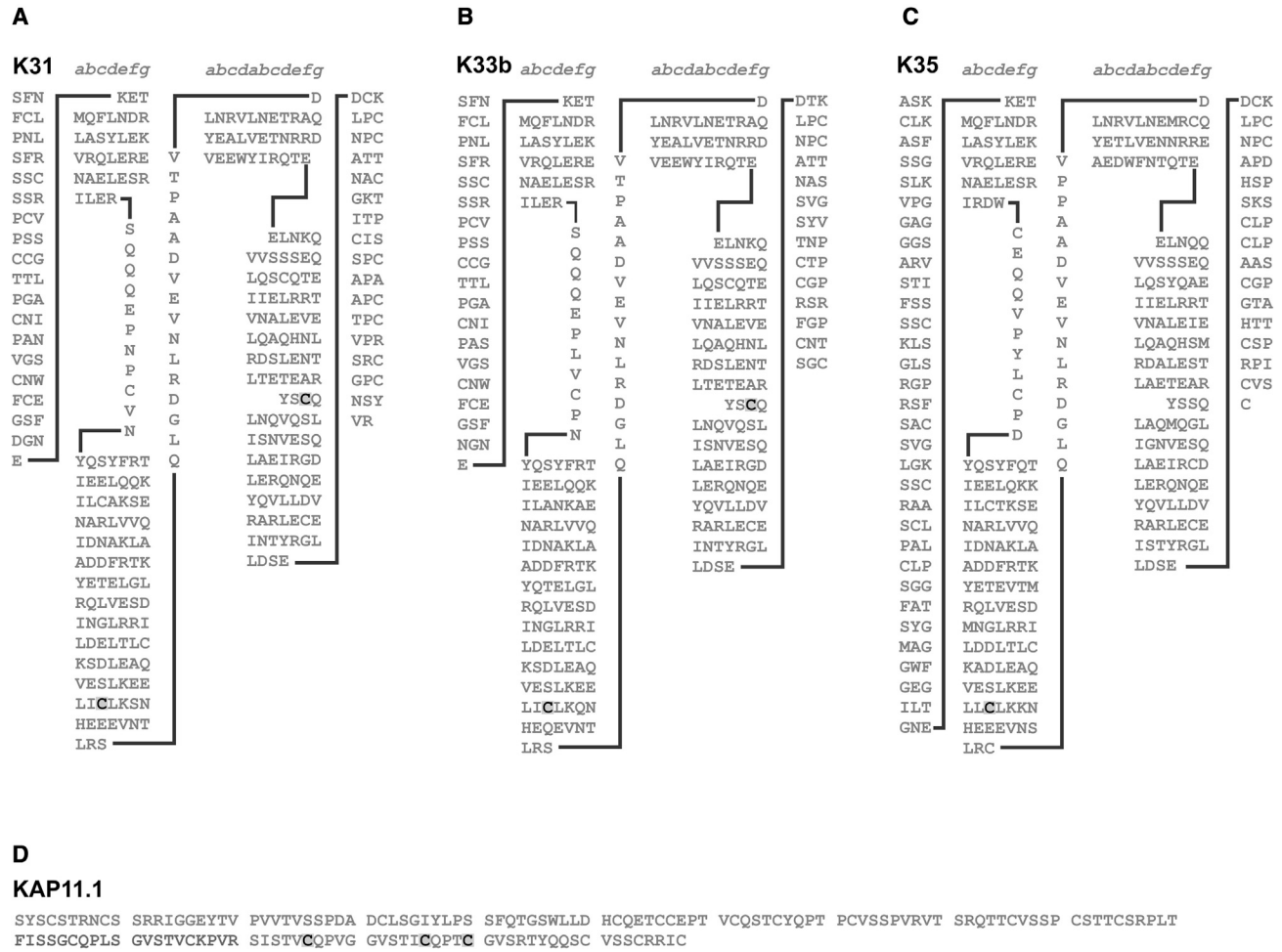

FIGURE 6 Keratins that show consistent labeling in the dry treatments and KAP11.1, which was labeled only in fiber stretch and holds conditions both in aqueous and dry conditions. (*A*) K31. (*B*) K33b. (*C*) K35, (*D*) KAP11.1. Labeled cysteines are highlighted and in bold.

with KAPs, though some theories hold that cysteines in the tail domain are involved in keratin-keratin crosslinking (29). In the early stages of follicle development, keratin-KAP interaction is most likely to be between K85 and KAP11.1, the expression of the latter starting in the mid-upper bulb region of the follicle (30). In the case of KAP11.1, three potential sites of disulfide bonding have been identified at cysteines 126, 136, and 140 (Table 2 *F*; Fig. 6 *D*). In addition to this, KAP interactions are also possible between KAP13.1 and KAP8.1 with K85. With the expression of keratin K35 starting around the same time as K85, followed shortly after by K31, these are also likely candidates for interactions with KAP11.1, KAP13.1, and KAP8.1.

Keratin 35 is an outlier

We identified a cysteine residue in the 1B rod domain of K35 that was more readily labeled than random but only under dry conditions (i.e., hydrogen-bond reinforcement) and only when fibers were stretched to break (Table 2 *G*; Fig. 6 *C*). While we do not understand

KAP2.3

TGSCCGPTFS SLSCGGGCLQ PCCYRDPCCC RPVSCQTVSR PVTFVPRCTR PICEPCRRPV CCDPCSLQEG CCRPITCCPT SCQAVVCRPC CWATTCCQPV
SVQCPCCRPT SCQPAPCSRT TCRTFRTSPC C

KAP3.2

ACCAPRCCSV RTGPATTICS SDKFCRCGVC LPSTCPHNIS LLQPTCCDNS PVPCYVPDTY VPTCFLLNSS HPTPGLSGIN LTTFIQPGCE NVCEPRC

FIGURE 7 KAPs with cysteines labeled when stretched for an extended period under water.

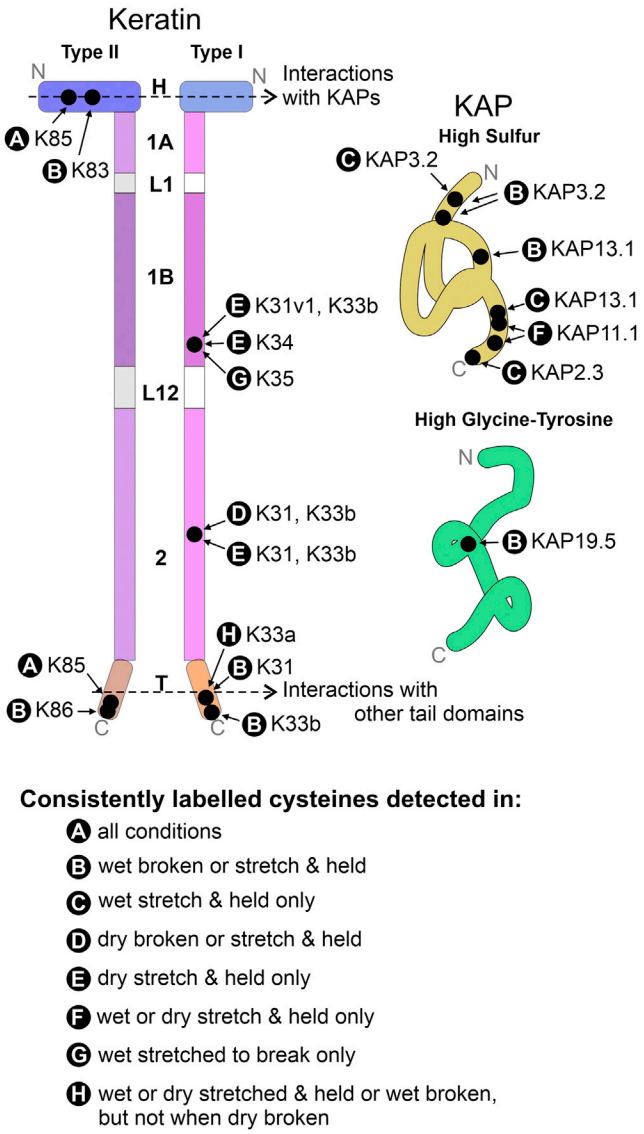

FIGURE 8 Summary of locations of consistently labeled cysteines under all conditions on generic keratin and KAP structures. Letters for test conditions as in Table 2. Colors and domain names as in Figs. 1 and 4 *A*. To see this figure in color, go online.

how this relates to either fiber mechanics or hair growth, it is worth noting that K35 is unusual in other ways. During fiber growth in the follicle bulb, K35 is the first type I keratin expressed in both the cortical and cuticular cell compartments (28,31), and its transient expression leads to a lower abundance than other type I keratins (32).

Disproportionately affected molecular locations change with water state

When stretching is carried out under wet conditions, in which hydrogen bonding had been disrupted, the cysteines disproportionally affected by tensile stress were those from the head domain of the type II keratin K83 and the tail domains of the type I keratins K31 and K33b (Table 2 *B*; Fig. 5). This is consistent with previous observations in the context of chemical accessibility. Of particular interest is the X-Pro-Cys repeat sequence in the type I keratin K31. This has previously been identified as a potential site of interaction between tail domains of keratins (26,29). In the case of the type II keratins, the cysteines in the longer head domains appear to be more accessible to reduction and alkylation than those in the shorter head domains of the type I keratins (26). This suggests that the head domains of the type II keratins, via their cysteine residues, are primarily involved in keratin-KAP interactions. This may be because these cysteine residues are more exposed to water in the fiber than those in the shorter head domains of the type I keratins.

Among the potential candidates for crosslinking with these keratins are the HS proteins KAP3.2 and KAP13.1 var1 and the HGT protein KAP19.5 (Table 2 *B*; Fig. 7), all of which were labeled under the same stretching conditions. Interestingly, the same cysteine in KAP 3.2 that had high accessibly to chemical damage (27) was also identified here (Fig. 7).

In contrast, when stretching to 25% extension was carried out in dry conditions, when the protein molecular structure is reinforced by protein-protein hydrogen bonds, the only cysteines consistently labeled were those coming from the 1B and 2 rod regions of the type I keratins (Table 2 *D*, and *E*; Fig. 6 *A* and *B*). In the case of these cysteines, 1B-87 in coil 1B of K33 var1 and K34 has been shown to be involved in crosslinking to the cysteine L1-9 of a type I keratin in mouse type I trichocyte keratins (33). Such a crosslink would be consistent with an A^{11} alignment of the heterodimers in the tetramer (26). Likewise, cysteine 2-90 in coil 2 of K31 and K33b has been shown to crosslink to cysteine 2-90 in another type I human in epithelial keratins and consistent with an A^{22} alignment in the tetramer (34). All of these cysteines have previously been shown to be readily accessible to reducing and alkylating agents (26). Thus, it would appear that stretching carried out under these conditions results in the breakage of disulfide bonds between the heterodimers in the tetramer.

KAP11.1 stands out from the many other KAPs

One protein that showed interesting behavior was KAP11.1 because three of its disulfide bonds, involving cysteines at positions 126, 136, and 140, were only labeled when tensioned to 25% for 2 min when either wet or dry and not when stretched to break for 10 min under the same conditions (Table 2 *F*; Fig. 6 *D*). One of the reasons for conducting the two different treatments, tensioning or stretched to break, was to determine whether the tensioning process would allow more disulfide bonds to break and reform if the stress was spread more evenly across the structure, i.e., which disulfide bonds are the most pliable. This would appear to be the case for the disulfide bonds involving these cysteines in KAP11.1.

CONCLUSIONS

This study on the effect on keratins in the cortex of intact wool fibers subject to stretching to break under wet or dry conditions has revealed the following:

- Our primary conclusion is that tensile stress breaks some disulfide bonds more readily than others and that which disulfide bonds and where they are located within keratins and KAPs depends on the rate of strain and the water state of the hair.
- Cysteines in the head and tail domain of K85 are disrupted under all stretching conditions.
- Stretching when hydrogen-bond disruption occurs, under wet conditions, results in the labeling of cysteines in the head domain of type II keratins most likely to be involved in keratin-KAP interactions, possibly because these are more exposed to water in the fiber.
- Stretching when hydrogen-bond disruption occurs, under wet conditions, results in the labeling of interactions in the tail domain of type I keratins most likely to be involved in keratin-keratin interactions.
- Stretching when the structure is maintained by hydrogen bonds, under dry conditions, was confined to the rod domains and primarily affects cysteines involved in interactions between heterodimers in the tetramers of the intermediate filament consistent with A_{11} and A_{22} alignments.
- In the early stages of follicle development, keratin-KAP interactions are most likely to be between K85 and two proteins, KAP11.1 and KAP13.1.

SUPPORTING MATERIAL

Supporting material can be found online at https://doi.org/10.1016/j.bpj.2022.04.029.

AUTHOR CONTRIBUTIONS

D.P.H., S.D.-C., and J.E.P. conceived the experiment. C.W., E.L., C.P., and D.P.H. carried out the fiber-stretching and sample-processing stages. S.D.-C. and J.E.P. carried out the MS stage. Data analysis and interpretation involved D.P.H., C.P., M.R., S.D.-C., and J.E.P. The manuscript was drafted by J.E.P. and D.P.H. with contributions, review, and edits by C.P., M.R. and S.D.-C.

DECLARATION OF INTERESTS

The authors declare no competing interests.

ACKNOWLEDGMENTS

We acknowledge advice and technical assistance from Peter Brorens, Ancy Thomas, Rachel Miller, Steve Gebbie, Robert Woods, and Lyall Bright from AgResearch. We thank Anita Grosvenor, Stefan Clerens, and Jolon Dyer from AgResearch and Steven Breakspear and Bernd Noecker (Kao Germany) for support and discussions that contributed to the study. Funding contributions to this study came from the Wool Research Organisation of New Zealand (WRONZ) and the New Zealand Government's Ministry for Business Innovation and Employment (MBIE) via the "New Materials from Wool" Partnership via Wool Industry Research, Ltd. and from AgResearch through its Smart and Sustainable Bio-based Materials Program (MBIE, Science strategic investment fund, contract number: C10X0710).

REFERENCES

1. Lim, Y. S., D. P. Harland, and T. L. Dawson, Jr. 2019. Wanted, dead and alive; why a multidisciplinary approach is needed to unlock hair treatment potential. *Exp. Dermatol.* 28:517–527. https://doi.org/10.1111/exd.13898.
2. Lim, Y.-S., D. P. Harland, and T. L. Dawson. 2018. Hair shaft formation and mitochondrial bioenergetics: combining biology, chemistry, and physics. *J. Cosmet. Sci.* 69:323–334.
3. Sinclair, R. D. 2007. Healthy hair: what is it? *J. Invest. Dermatol. Symp. Proc.* 12:2–5. https://doi.org/10.1038/sj.jidsymp.5650046.
4. Quinlan, R. A., E. H. Bromley, and E. Pohl. 2015. A silk purse from a sow's ear — bioinspired materials based on α-helical coiled coils. *Curr. Opin. Cell Biol.* 32:131–137. https://doi.org/10.1016/j.ceb.2014.12.010.
5. McKittrick, J., P. Y. Chen, …, M. A. Meyers. 2012. The structure, functions, and mechanical properties of keratin. *JOM.* 64:449–468. https://doi.org/10.1007/s11837-012-0302-8.
6. Cera, L., G. M. Gonzalez, …, K. K. Parker. 2021. A bioinspired and hierarchically structured shape-memory material. *Nat. Mater.* 20:242–249. https://doi.org/10.1038/s41563-020-0789-2.
7. Tardy, B. L., B. D. Mattos, …, O. J. Rojas. 2021. Deconstruction and reassembly of renewable polymers and biocolloids into next generation structured materials. *Chem. Rev.* 121:14088–14188. https://doi.org/10.1021/acs.chemrev.0c01333.
8. Wang, J., D. Lü, …, M. Long. 2014. Mechanomics: an emerging field between biology and biomechanics. *Protein Cell.* 5:518–531. https://doi.org/10.1007/s13238-014-0057-9.
9. Harland, D. P., and J. E. Plowman. 2018. Development of hair fibres. *In* Advances in Experimental Medicine and Biology, the Hair Fibre: Proteins, Structure and Development. J. E. Plowman, D. P. Harland, and S. Deb Choudhury, eds. Springer, New York, pp. 109–154.
10. Bornschlögl, T., L. Bildstein, …, N. Baghdadli. 2016. Keratin network modifications lead to the mechanical stiffening of the hair follicle fiber. *Proc. Natl. Acad. Sci. U S A.* 113:5940–5945. https://doi.org/10.1073/pnas.1520302113.
11. Eckhart, L., L. D. Valle, …, E. Tschachler. 2008. Identification of reptilian genes encoding hair keratin-like proteins suggests a new scenario for the evolutionary origin of hair. *Proc. Natl. Acad. Sci. U S A.* 105:18419–18423. https://doi.org/10.1073/pnas.0805154105.
12. Gillespie, J. M. 1990. The proteins of hair and other hard α-keratins. *In* Cellular and Molecular Biology of Intermediate Filaments. R. D. Goldman and P. M. Steinert, eds. Plenum Press, New York, pp. 95–128.
13. Cloete, E., N. P. Khumalo, and M. N. Ngoepe. 2020. Understanding curly hair mechanics: fiber strength. *J. Invest. Dermatol.* 140:113–120. https://doi.org/10.1016/j.jid.2019.06.141.
14. Meredith, R. 1957. 14—rigidity, moisture and fibre structure. *J. Textile Inst. Trans.* 48:T163–T174. https://doi.org/10.1080/19447025708660079.
15. Breakspear, S., B. Noecker, and C. Popescu. 2019. Relevance and evaluation of hydrogen and disulfide bond contribution to the mechanics of hard α-keratin fibers. *J. Phys. Chem. B.* 123:4505–4511. https://doi.org/10.1021/acs.jpcb.9b01690.

16. Langbein, L., and J. Schweizer. 2005. Keratins of the human hair follicle. *Int. Rev. Cytol.* 243:1–78. https://doi.org/10.1016/s0074-7696(05)43001-6.

17. Yu, Z., S. W. Gordon, …, A. J. Pearson. 2009. Expression patterns of keratin intermediate filament and keratin associated protein genes in wool follicles. *Differentiation.* 77:307–316. https://doi.org/10.1016/j.diff.2008.10.009.

18. Fraser, R. D., and D. A. Parry. 2005. The three-dimensional structure of trichocyte (hard α-) keratin intermediate filaments: features of the molecular packing deduced from the sites of induced cross-links. *J. Struct. Biol.* 151:171–181. https://doi.org/10.1016/j.jsb.2005.06.003.

19. Fraser, R. B., and D. A. Parry. 2017. Intermediate filament structure in fully differentiated (oxidised) trichocyte keratin. *J. Struct. Biol.* 200:45–53. https://doi.org/10.1016/j.jsb.2017.09.003.

20. Harland, D. P., and A. J. McKinnon. 2018. Macrofibril formation. *In* Advances in Experimental Medicine and Biology, the Hair Fibre: Proteins, Structure and Development. J. E. Plowman, D. P. Harland, and S. Deb Choudhury, eds. Springer, New York, pp. 155–169.

21. Caldwell, J. P., D. N. Mastronarde, …, W. G. Bryson. 2005. The three-dimensional arrangement of intermediate filaments in Romney wool cortical cells. *J. Struct. Biol.* 151:298–305. https://doi.org/10.1016/j.jsb.2005.07.002.

22. Harland, D. P., R. J. Walls, …, F. Bell. 2014. Three-dimensional architecture of macrofibrils in the human scalp hair cortex. *J. Struct. Biol.* 185:397–404. https://doi.org/10.1016/j.jsb.2014.01.010.

23. Harland, D. P., J. L. Woods, …, J. A. Vernon. 2007. Arrangement of trichokeratin intermediate filaments and matrix in the cortex of merino wool. *J. Struct. Biol.* 173:29–37. https://doi.org/10.1016/j.jsb.2010.08.009.

24. Kadir, M., X. Wang, …, C. Popescu. 2017. The structure of the "amorphous" matrix of keratins. *J. Struct. Biol.* 198:116–123. https://doi.org/10.1016/j.jsb.2017.04.001.

25. Woods, J. L., and D. F. G. Orwin. 1987. Wool proteins of New Zealand romney sheep. *Aust. J. Biol. Sci.* 40:1–14. https://doi.org/10.1071/bi9870001.

26. Plowman, J. E., R. E. Miller, …, S. Deb Choudhury. 2021. A detailed mapping of the readily accessible disulphide bonds in the cortex of wool fibres. *Proteins.* 89:708–720. https://doi.org/10.1002/prot.26053.

27. Deb-Choudhury, S., J. E. Plowman, …, D. P. Harland. 2015. Mapping the accessibility of the disulfide crosslink network in the wool fiber cortex. *Proteins: Struct. Funct. Bioinformatics.* 83:224–234. https://doi.org/10.1002/prot.24727.

28. Langbein, L., M. A. Rogers, …, J. Schweizer. 2001. The catalog of human hair keratins. II. Expression of the six type II members in the hair follicle and the combined catalog of human type I and II keratins. *J. Biol. Chem.* 276:35123–35132. https://doi.org/10.1074/jbc.M103305200.

29. Parry, D. A., and A. North. 1998. Hard α-keratin intermediate filament chains: substructure of the N- and C-terminal domains and the predicted structure and function of the C-terminal domains of type I and type II chains. *J. Struct. Biol.* 122:67–75. https://doi.org/10.1006/jsbi.1998.3967.

30. Rogers, M. A., L. Langbein, …, J. Schweizer. 2002. Characterization of a first domain of human high glycine-tyrosine and high sulfur keratin-associated protein (KAP) genes on chromosome 21q22.1. *J. Biol. Chem.* 277:48993–49002. https://doi.org/10.1074/jbc.m206422200.

31. Langbein, L., M. A. Rogers, …, J. Schweizer. 1999. The catalog of human hair keratins. I. Expression of the nine type I members in the hair follicle. *J. Biol. Chem.* 274:19874–19884. https://doi.org/10.1074/jbc.274.28.19874.

32. Plowman, J. E., D. P. Harland, …, D. R. Scobie. 2015. The proteomics of wool fibre morphogenesis. *J. Struct. Biol.* 191:341–351. https://doi.org/10.1016/j.jsb.2015.07.005.

33. Wang, H., D. A. Parry, …, P. M. Steinert. 2000. In vitro assembly and structure of trichocyte keratin intermediate filaments: a novel role for stabilization by disulfide bonding. *J. Cell Biol.* 151:1459–1468. https://doi.org/10.1083/jcb.151.7.1459.

34. Steinert, P. M., and D. A. D. Parry. 1993. The conserved H1 domain of the type II keratin 1 chain plays an essential role in the alignment of nearest neighbor molecules in mouse and human keratin 1/keratin 10 intermediate filaments at the two- to four-molecule level of structure. *J. Biol. Chem.* 268:2878–2887. https://doi.org/10.1016/s0021-9258(18)53855-2.